Figures and figure supplements

Influenza-virus membrane fusion by cooperative fold-back of stochastically induced hemagglutinin intermediates

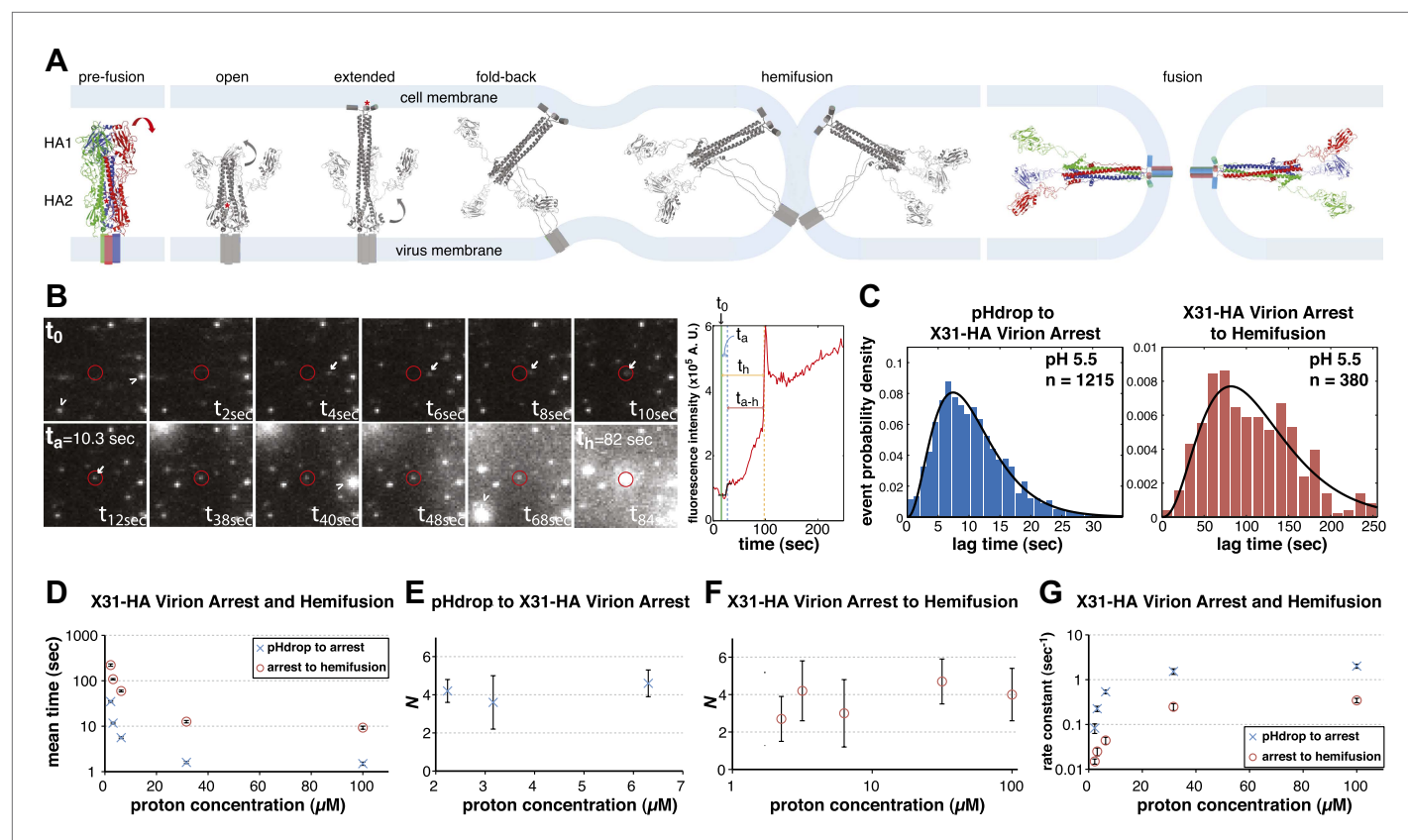**Tijana Ivanovic, et al.**

Figure 1. Single-virion analysis of fusion-promoting conformational change in influenza virus HA. (**A**) Hydrophobic fusion peptide (red asterisk) is initially inserted into a pocket near the trimer threefold axis. HA assumes an 'open' conformation upon proton binding allowing fusion-peptide release and membrane insertion. The fold-back of the extended intermediate causes hemifusion. The known pre-fusion and post-fusion HA structures are colored, and the inferred structural transitions are showed in gray. (**B**) *Left*: Tile view from pH drop (t_0) of a virion initially displaying directed motion (white arrow) followed by arrest (t_a) then hemifusion (t_h). Red circle marks the final virion location. Arrowheads mark two virions that were arrested at pH drop and hemifused at or just before $t_{40 s}$ and $t_{68 s}$ respectively. *Right*: Fluorescence trace of the virion circled in (**A**) (red line), line fitting the timing of virion arrest at its target location (black line) and parameters t_0 (green vertical line), t_a (blue horizontal line) and t_h (orange horizontal line) and arrest to hemifusion, t_{a-h} (dark orange horizontal line). (**C**) $t_{lag}^{(pHdrop-arrest)}$ for all virions for which arrest values could be derived (*left*) and $t_{lag}^{(arrest-hemifusion)}$ for all virions for which both arrest and hemifusion values could be derived (*right*) with gamma-distribution fit (black line). Data are pooled from three independent experiments. (**D**) Mean $t_{lag}^{(pHdrop-arrest)}$ and $t_{lag}^{(arrest-hemifusion)}$. Error bars represent the standard error of the mean. (**E**) and (**F**) N derived from fitting $t_{lag}^{(pHdrop-arrest)}$ (**E**) and $t_{lag}^{(arrest-hemifusion)}$ (**F**) with gamma probability density. (**G**) Rate constants derived from fitting $t_{lag}^{(arrest-hemifusion)}$ and $t_{lag}^{(pHdrop-arrest)}$ with gamma probability density and keeping N fixed (N = 3) for both processes. (**B–G**) X31-HA virions have X31 HA in otherwise Udorn genetic background. Data shown are from representative experiments performed on the same day (n = 50 to 150) unless indicated that multiple experiments were pooled. Error bars represent 95% confidence interval for gamma fit-derived values unless otherwise indicated. Please refer to *Figure 1—figure supplement 1* for all histogram and gamma-distribution fit data plotted in (**D–G**).
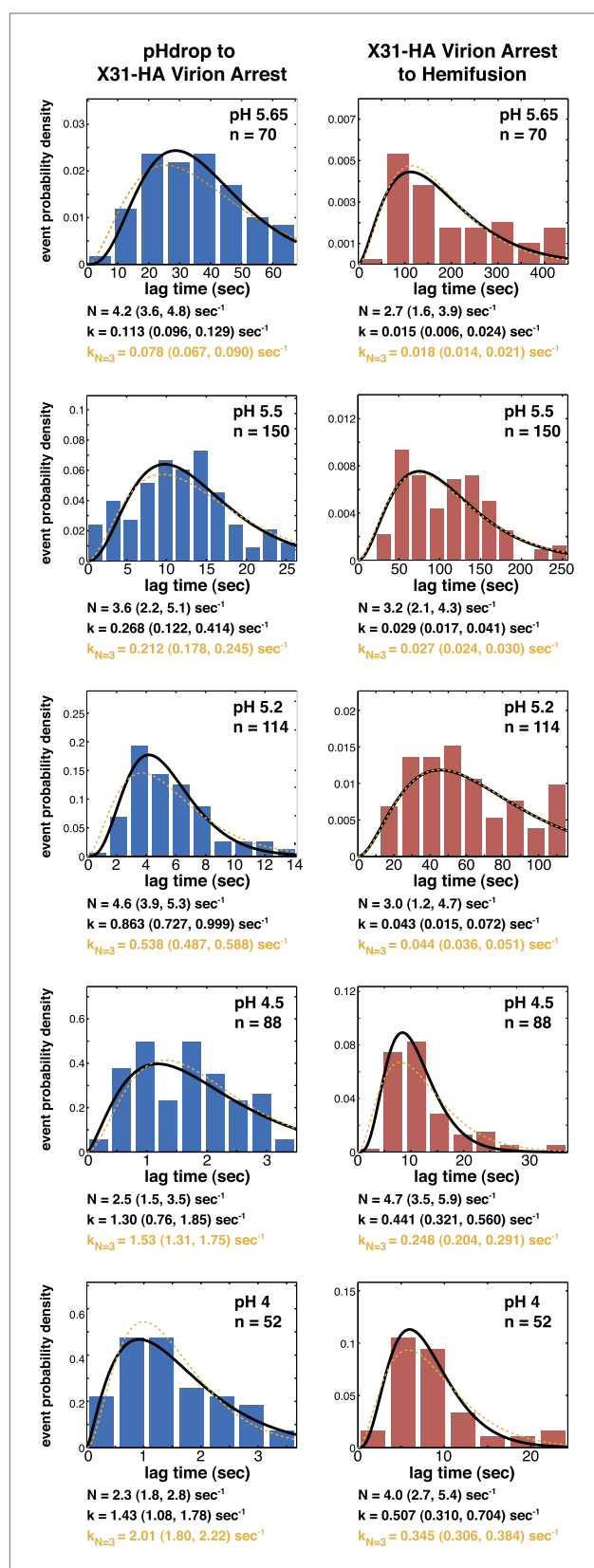DOI: 10.7554/eLife.00333.003

Figure 1—figure supplement 1. Histograms of $t_{lag}^{(pHdrop-arrest)}$ (*left*) and $t_{lag}^{(arrest-hemifusion)}$ (*right*) for X31-HA virions. Data are fitted with
Figure 1—figure supplement 1. Continued on next page

Figure 1—figure supplement 1. Continued

gamma-probability density where both N and k were fitted (black line) or N was fixed (N = 3) (orange line). Fit-derived values are indicated below each histogram in corresponding black and orange font colors. Parentheses indicate 95% confidence interval for each fit-derived value.
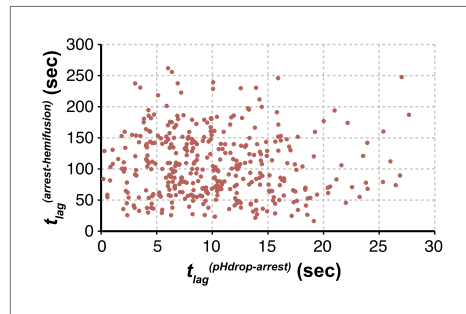
Figure 2. Virion arrest and hemifusion lag times are uncorrelated. $t_{lag}^{(arrest–hemifusion)}$ vs $t_{lag}^{(pHdrop–arrest)}$ for X31-HA virions at pH 5.5 (n = 380). Data are pooled from three independent experiments also shown in *Figure 1C*, *Table 1* and *Figure 4A,B* (X31–HA).
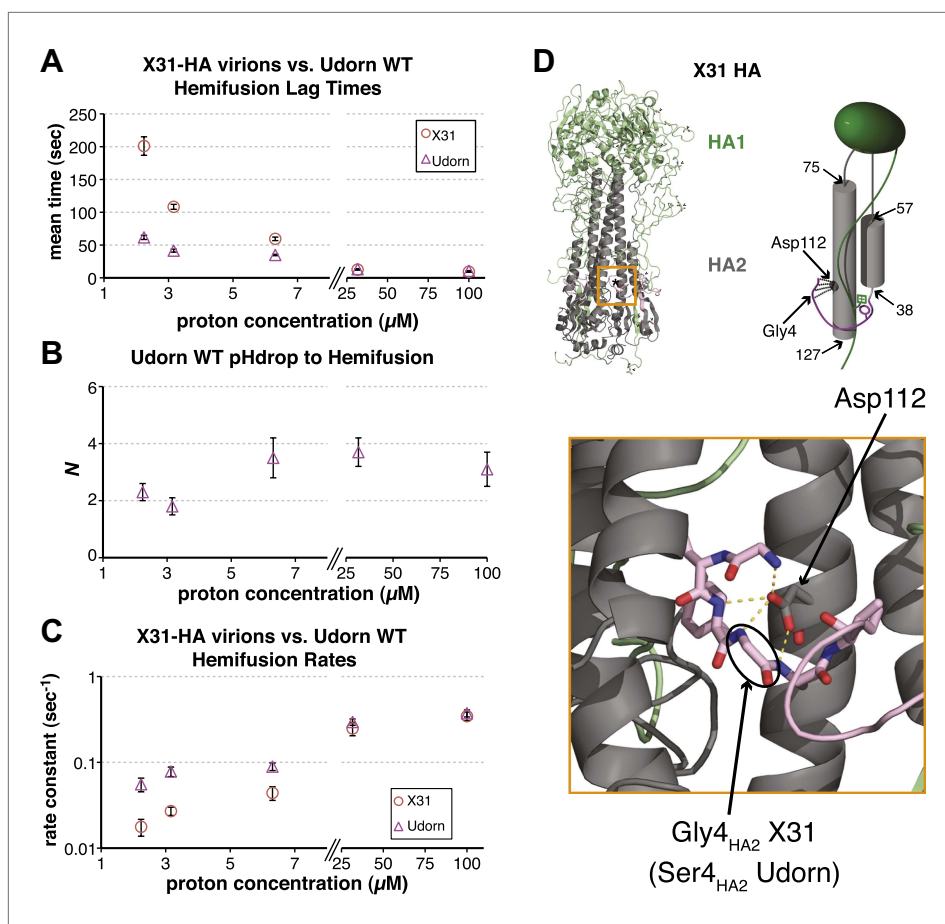
Figure 3. Udorn virions have accelerated hemifusion kinetics. (**A**) Mean $t_{lag}^{(pHdrop-hemifusion)}$ for Udorn and mean $t_{lag}^{(arrest-hemifusion)}$ for X31-HA virions. Error bars represent the standard error of the mean. (**B**) N derived from fitting $t_{lag}^{(pHdrop-hemifusion)}$ with gamma probability density. (**C**) Rate constants derived from fitting $t_{lag}^{(pHdrop-arrest)}$ for Udorn and $t_{lag}^{(arrest-hemifusion)}$ for X31-HA virions with gamma probability density and keeping each N fixed ($N = 3$). (**B–C**) Error bars represent 95% confidence interval for gamma fit-derived values. (**A–C**) Data shown are from representative experiments performed on the same day (n = 50 to 350). Please refer to *Figure 3—figure supplement 1* for all histogram and gamma-distribution fit data plotted in (**A–C**). (**D**) *Top left*: Ribbon representation of X31-HA trimer (*Weis et al., 1990*) showing positions of all residues that differ in Udorn-HA (arrowhead) including Gly4$_{HA2}$ (asterisk). *Top right*: Cartoon of an HA monomer emphasizing Asp112$_{HA2}$-fusion peptide hydrogen bond network and showing positions of residues along the HA$_2$ chain. *Bottom*: Close-up of the Asp112$_{HA2}$-fusion peptide network (region marked with an orange square on top left).
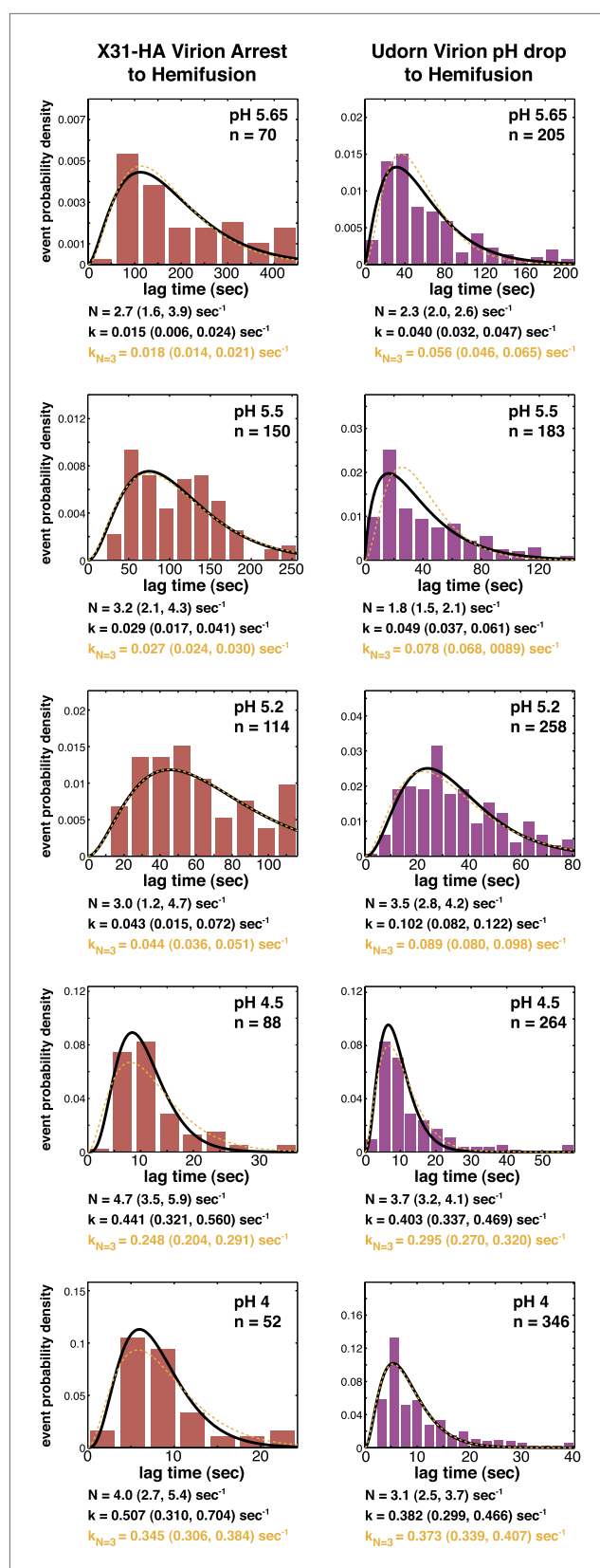DOI: 10.7554/eLife.00333.010

Figure 3—figure supplement 1. Histograms of $t_{lag}^{(arrest-hemifusion)}$ for X31-HA virions (*left*) and of $t_{lag}^{(pHdrop-hemifusion)}$ for Udorn WT virions (*right*). Data are fitted with gamma-probability density where both *Figure 3—figure supplement 1. Continued on next page*

Figure 3—figure supplement 1. Continued

N and k were fitted (black line) or N was fixed (N = 3) (orange line). Fit-derived values are indicated below each histogram in corresponding black and orange font colors. Parentheses indicate 95% confidence interval for each fit-derived value.
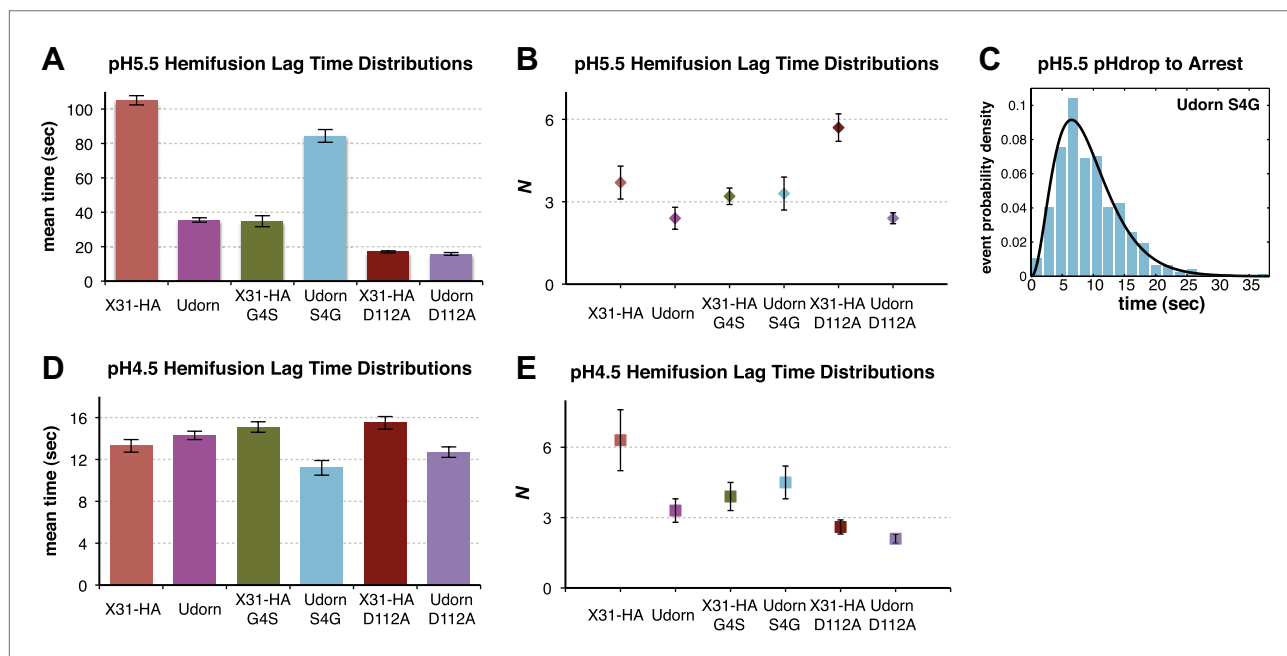DOI: 10.7554/eLife.00333.011

Figure 4. Fusion-peptide release from its pre-fusion pocket is a rate-limiting fusion-inducing molecular rearrangement in the physiologically relevant pH regime. (**A**) pH 5.5, mean $t_{lag}^{(arrest–hemifusion)}$ for X31-HA WT, $S4G_{HA2}^{Udorn}$ and mean $t_{lag}^{(pHdrop–hemifusion)}$ for Udorn WT, $G4S_{HA2}^{X31}$, $D112A_{HA2}^{Udorn}$ and $D112A_{HA2}^{X31}$. (**B**) N derived from gamma-probability-density fits of the data analyzed also in (**A**). (**C**) Histogram of $t_{lag}^{(arrest–hemifusion)}$ distribution for $S4G_{HA2}^{Udorn}$ virions at pH 5.5 with the gamma-probability-density fit (black line). (**D**) pH 4.5, mean $t_{lag}^{(pHdrop–hemifusion)}$ for indicated virions. (**E**) N derived from gamma-probability-density fits of the data analyzed also in (**D**). (**A–E**) Data shown are from pooled independent experiments (3, for Udorn and X31-HA WT virions, and 2, for Udorn and X31-HA mutant virions; n = 150 to 900). Error bars represent the standard error of the mean (**A** and **D**) or the 95% confidence interval for gamma fit-derived values (**B** and **E**). Please refer to *Figure 4—figure supplement 1* for all histogram and gamma-distribution fit data plotted in (**A**, **B**, **D** and **E**).
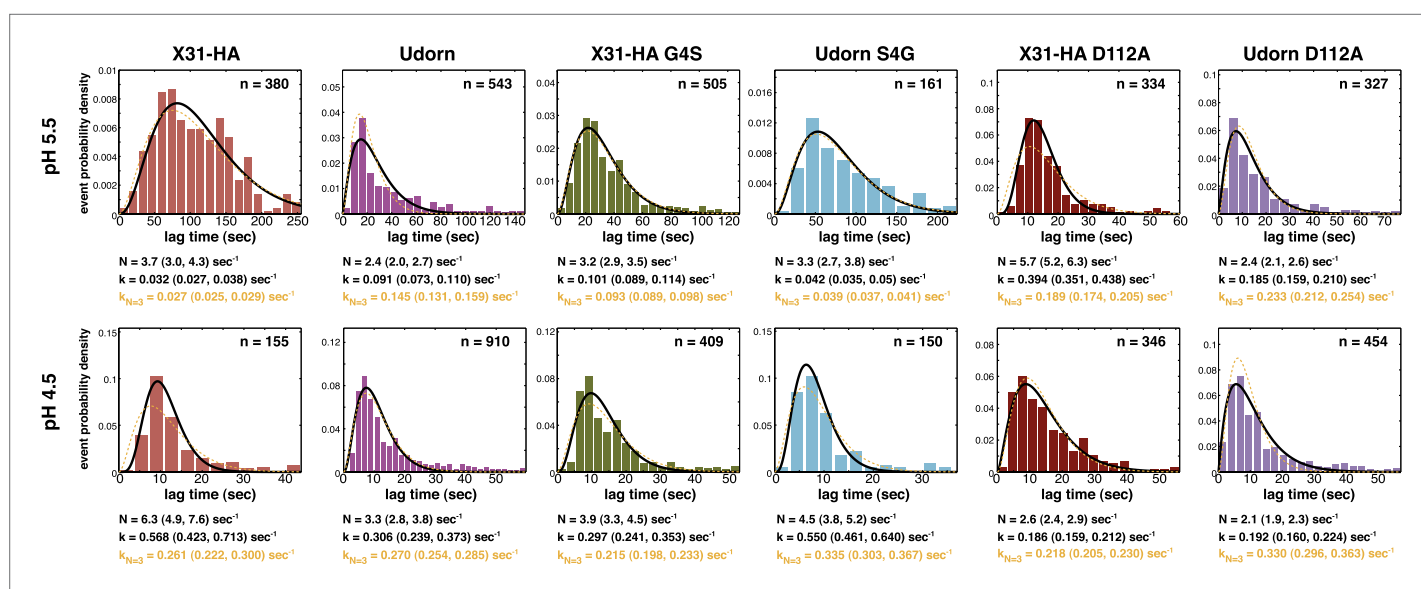DOI: 10.7554/eLife.00333.012

Figure 4—figure supplement 1. Histograms of $t_{lag}^{(arrest-hemifusion)}$ distributions for X31-HA WT, $S4G_{HA2}^{Udorn}$ virions and of $t_{lag}^{(pHdrop-hemifusion)}$ for Udorn WT, $G4S_{HA2}^{X31}$, $D112A_{HA2}^{Udorn}$ and $D112A_{HA2}^{X31}$ at pH 5.5 (*top*). Histograms of $t_{lag}^{(pHdrop-hemifusion)}$ for all virions at pH 4.5 (*bottom*). Data are fitted with gamma-probability density where both *N* and *k* were fitted (black line) or *N* was fixed (*N* = 3) (orange line). Fit-derived values are indicated below each histogram in corresponding black and orange font colors. Parentheses indicate 95% confidence interval for each fit-derived value.
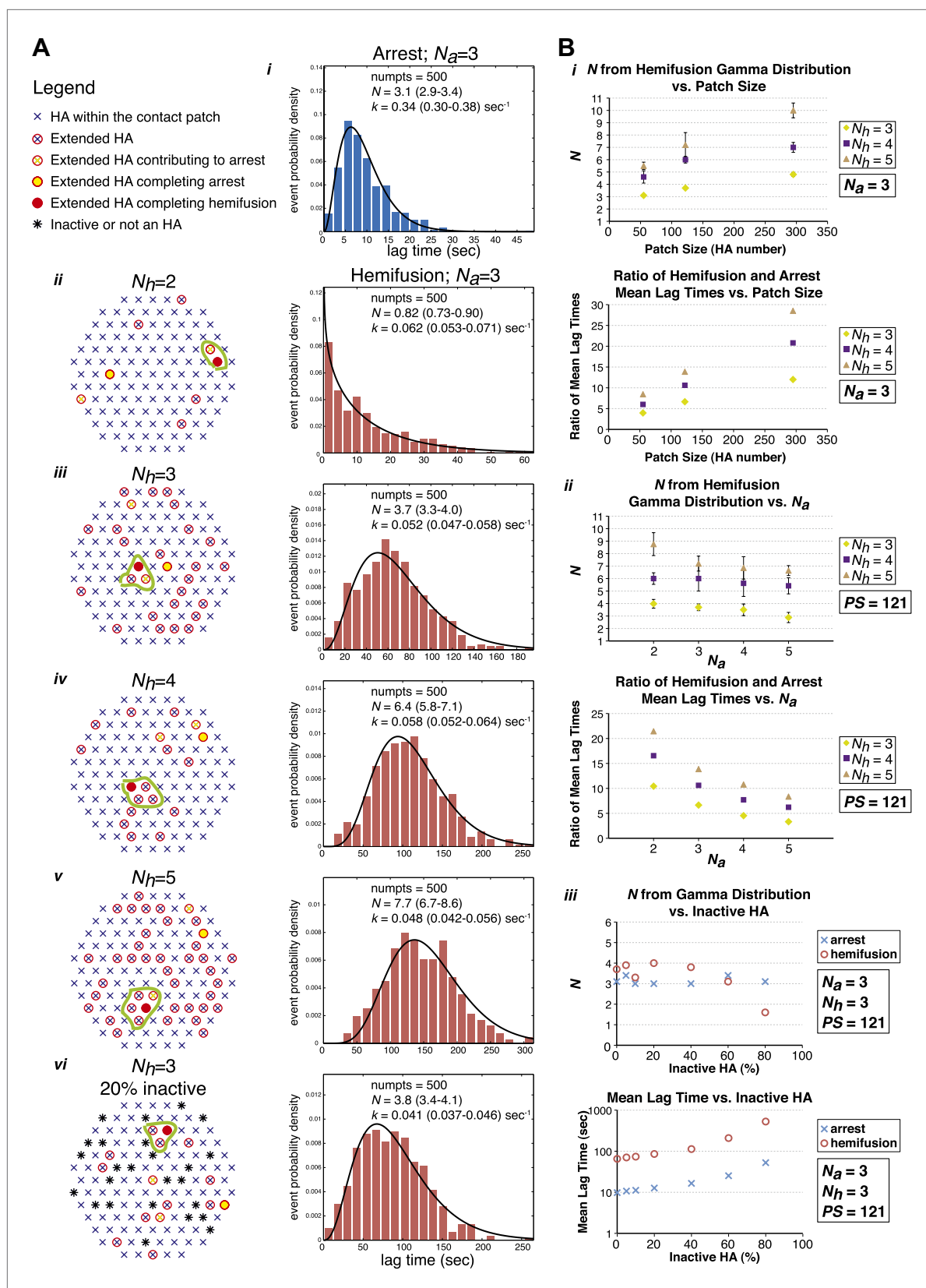DOI: 10.7554/eLife.00333.013

Figure 5. Computer simulation of the proposed model for HA-mediated membrane fusion. (**A**) *Left*: A contact patch containing 121 HA trimers and examples of individual virions and their contact-area HAs that have extended and inserted their fusion peptides into the target membrane by the time of *Figure 5. Continued on next page*

Figure 5. Continued

hemifusion, for simulated N_h values of 2–5 and assuming either a contact patch consisting solely of active HAs (*ii–v*) or containing 20% inactive HAs randomly distributed throughout the contact area (*vi*). The neighboring HA clusters inducing hemifusion in each case are circled in green. *Right:* N_a = 3 and patch size = 121 containing either 0% or 20% inactive HAs as indicated in the corresponding diagrams; simulation-derived $t_{lag}^{(pHdrop–arrest)}$ distributions (*i*) and $t_{lag}^{(arrest–hemifusion)}$ distributions for N_h = 2–5 (*ii–vi*) along with gamma-distribution fits (black curves) and fit-derived values for N and k. Parentheses indicate 95% confidence interval for each fit-derived value. We collected data for 500 virions in each example. (**B**) (*i*) N_a = 3; effect of patch size (PS) and N_h either on gamma-fit-derived values for N from hemifusion lag-time distributions (*top*) or on ratios of hemifusion and virion arrest mean lag times (*bottom*). (*ii*) Patch size = 121; effect of N_a and N_h either on gamma-fit-derived values for N from hemifusion lag-time distributions (*top*) or on ratios of hemifusion and virion arrest mean lag times (*bottom*). (*iii*) N_a = 3, N_h = 3, patch size = 121; gamma-fit-derived N values (*top*) and mean lag times (*bottom*) for arrest and hemifusion at a range of inactive HA concentrations. Data shown are averages, and error bars, when included, represent standard deviation for five independent simulations each performed for 500 virions. For MATLAB script and accompanying functions please refer to ***Source code 1***.
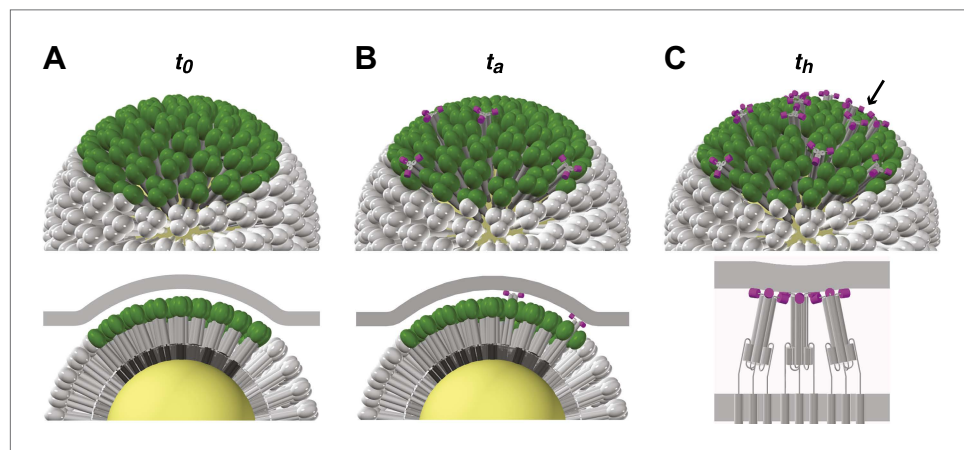
Figure 6. Stages of HA-mediated membrane fusion. Virion dimensions in the diagram are based on a spherical particle, 55 nm in membrane-to-membrane diameter (***Calder et al., 2010***). There are approximately 50 trimers in the contact area between the virus and the target cell, shown in green (HA$_1$) and gray (HA$_2$); the trimers outside of the contact area are shown in white. The contact area illustrated represents a lower limit, and the contact area for the somewhat elongated particles in our current experiments can likely accommodate up to approximately 120 HA trimers (see 'Results' and 'Materials and methods'). For clarity we present a virion surface containing only HA, but the conclusions we draw are independent of specific HA arrangement and potential irregularities in this region of contact (see ***Figure 5***). We have also not included the target membrane in the perspective views (top), nor have we depicted the sialic-acid receptors in the cross-section views (bottom). The t_0, t_a and t_h labels are included to correlate the molecular transitions depicted in the model with the events defined in ***Figure 1B***. (**A**) Virion engages a target membrane by HA-receptor interactions but can still move freely relative to the target-membrane area of contact. (**B**) Fusion peptides of several independent HA trimers have inserted into the target-membrane surface, immobilizing the virion on the target-cell surface. (**C**) Engagement of fusion peptides from three neighboring HA trimers allows subsequent rearrangements leading to hemifusion. HA$_1$s are left out for clarity from the bottom panel, which shows three neighboring trimers about to fold back.